

June 1997

# Determination of the CKM unitarity triangle by $B \rightarrow X_d \ell^+ \ell^-$ decay

**L. T. Handoko \***

Department of Physics, Hiroshima University  
1-3-1 Kagamiyama, Higashi Hiroshima - 739, Japan

## Abstract

We attempt to extract the angle  $\gamma$  of the Cabibbo-Kobayashi-Maskawa matrix by the inclusive  $B \rightarrow X_d \ell^+ \ell^-$  decay in the Standard Model. An independent information for the angle is coming out from the non-trivial contribution due to CP violation factor, which induces CP asymmetry in the channel. The decay rate and asymmetries are examined with including the long-distance contributions due to vector-mesons as well as the momentum dependences of the vector-mesons, that would reduce the long-distance backgrounds in the process. It is shown that in the low dilepton invariant mass region, the branching-ratio for any dilepton final states and the lepton polarization asymmetry for dimuon final state would be sensitive to the CP violation contribution in addition to the trivial CP asymmetry. On the other hand, in the high dilepton invariant mass region, the contribution is tiny that make it a good probe to confirm the measurement of  $x_d$  in addition to the present data from  $B_d^0 - \bar{B}_d^0$  mixing.

---

\*On leave from P3FT-LIPI, Indonesia. E-mail address : handoko@theo.phys.sci.hiroshima-u.ac.jp

# 1 Introduction

The hope that  $B \rightarrow X_s \ell^+ \ell^-$  decay will be within experimental reach in the near future [1] encourage us to consider another similar channel,  $B \rightarrow X_d \ell^+ \ell^-$  decay. These decays are important probes of the effective Hamiltonian governing the flavor-changing neutral current (FCNC) transition  $b \rightarrow q \ell^+ \ell^-$ , with  $q = s$  or  $d$  and  $\ell$ 's denote leptons, as written below [2],

$$\begin{aligned} \mathcal{H}_{\text{eff}} = & \frac{G_F \alpha}{\sqrt{2} \pi} V_{tq}^* V_{tb} \left\{ C_9^{\text{eff}} [\bar{q} \gamma_\mu L b] [\bar{\ell} \gamma^\mu \ell] + C_{10} [\bar{q} \gamma_\mu L b] [\bar{\ell} \gamma^\mu \gamma_5 \ell] \right. \\ & \left. - 2 C_7^{\text{eff}} \left[ \bar{q} i \sigma_{\mu\nu} \frac{\hat{q}^\nu}{\hat{s}} (R + \hat{m}_q L) b \right] [\bar{\ell} \gamma^\mu \ell] \right\}. \quad (1) \end{aligned}$$

where  $L/R \equiv (1 \mp \gamma_5)/2$ ,  $q^\mu$  denotes four-momentum of the dilepton and  $s = q^2$ . Notations with hat on the top means it is normalized with  $m_b$ .

However, in the present paper the interest is focused on the  $b \rightarrow d \ell^+ \ell^-$  decay, since theoretically the channel is more interesting, that is the matrix elements contains un-negligible terms induced by continuum part of  $u\bar{u}$  and  $c\bar{c}$  loops, proportional to  $V_{ud}^* V_{ub}$  and  $V_{cd}^* V_{cb}$  [5]. These terms, should give non-trivial contributions and induce CP violation in the channel, that is also related directly with the length  $r$  as well as the angle  $\gamma$  of Cabibbo-Kobayashi-Maskawa (CKM) unitarity triangle in Fig. 1. In this meaning, for example, the radiative  $B \rightarrow X_d \gamma$  decay is not so useful since it gives only information for the length  $x$  that have already been measured well by  $B_d^0 - \bar{B}_d^0$  mixing. On the other hand, in the  $b \rightarrow s \ell^+ \ell^-$  decay, the factor which we call CP violation factor ( $C_9^{\text{CP}}$ ) throughout this paper, is strongly suppressed due to the unitarity of CKM matrix.

On the other hand, non-perturbative effects in the rare  $B$  decays are tiny, less than few percents as shown in [3] by using heavy-quark effective theory approach<sup>1</sup>. In this meaning, generally rare  $B$  decays are clean processes to extract the CKM matrix elements. In the analysis, we also utilize the experimental value of  $B_d^0 - \bar{B}_d^0$

---

<sup>1</sup>Remark that the approach is reliable only in the low region of dilepton mass, but it is sufficient to justify the statement. Because the total distributions would be smaller and becoming zero as coming near to the high region of dilepton mass.

mixing which is usually called  $x_d$ . Then, in principle, we can determine the angle  $\gamma$  of CKM unitarity triangle as an independent measurement.

The purpose of this paper is to give an independent measurement for the angle  $\gamma$  of the CKM unitarity triangle in the Standard Model (SM) by observing the channel with taking into account the  $q$ -dependence of  $\gamma - V$  transition in the long-distance (LD) contributions due to vector-mesons ( $V$ 's) [8] as well as the  $C_9^{\text{CP}}$  contribution. It is well known that including  $q$ -dependence of  $\gamma - V$  transition, which has not been considered in the previous papers, will reduce the background due to LD contributions [9]. Remark here that in a recent paper [10], it is claimed that by keeping the photon propagator as  $-i g^{\mu\nu}/q^2$ , the LD background could be dominant, then makes it difficult to extract the short distance (SD) information. However, we have re-checked that  $1/q^2$  dependence must be canceled by the vacuum polarization tensor  $\Pi_{\mu\nu}$  which generally can be parametrized as  $\sim (g_{\mu\nu} q^2 - q_\mu q_\nu)$  as a consequence of current conservation [4].

This paper is organized as follows. First we briefly describe the non-trivial contributions due to resonances and continuums from  $u\bar{u}$  and  $c\bar{c}$  loops which induce the  $C_9^{\text{CP}}$ . Next we consider the phenomenological of the contributions as well as its relation with the CKM unitarity triangle. Before going to summary, the decay rate and asymmetries, i.e. forward-backward (FB) asymmetry ( $\bar{\mathcal{A}}_{\text{FB}}$ ), CP asymmetry ( $\bar{\mathcal{A}}_{\text{CP}}$ ) and lepton-polarization (LP) asymmetry ( $\bar{\mathcal{A}}_{\text{LP}}$ ) in the process, are discussed. Lastly, we give summary and discussion.

## 2 Resonances and CP violation factor contributions

The effective Hamiltonian in Eq. (1) describes both inclusive  $b \rightarrow q \ell^+ \ell^-$  decays by replacing  $q$  with  $s$  or  $d$  quarks respectively. In the SM, the QCD corrected Wilson coefficients enter in the physical decay amplitude above have been calculated up to next-to leading order (NLO) for  $C_9^{\text{eff}}$  and leading order (LO) for  $C_7^{\text{eff}}$  [6], while  $C_{10}$  does not receive any correction at all. Remind that the contribution of  $u\bar{u}$

loop in  $C_7^{\text{eff}}$  is cancelled because of the GIM mechanism and the function in the magnetic moment form factor is proportional to  $(m_i/M_W)^2 \sim 0$  for  $u$  and  $c$  quarks [11]. Otherwise, some corrections due to  $u\bar{u}$  and  $c\bar{c}$  continuums and the resonances of vector-mesons will enter only in the coefficient  $C_9^{\text{eff}}$ .

Before going to give an expression for  $C_9^{\text{eff}}$ , let us mention the operators govern the  $b \rightarrow q u^i \bar{u}^i$  processes, which are related with  $u\bar{u}$  and  $c\bar{c}$  loops,

$$\mathcal{O}_1 = (\bar{q}_\alpha \gamma_\mu L b_\alpha) \sum_{i=1,2} (\bar{u}_\beta^i \gamma^\mu L u_\beta^i) , \quad (2)$$

$$\mathcal{O}_2 = (\bar{q}_\alpha \gamma_\mu L b_\beta) \sum_{i=1,2} (\bar{u}_\beta^i \gamma^\mu L u_\alpha^i) , \quad (3)$$

after doing Fierz transformation. Here,  $u^1 = u$ ,  $u^2 = c$  and the lower suffixes denote the color. For  $q = s$ ,  $u\bar{u}$  loop contribution has been neglected as done in [2, 6], but for  $q = d$  the situation is quite different. The reason is, both operators above are proportional to CKM matrix element  $V_{u^i q}^* V_{u^i b}/V_{tq}^* V_{tb}$  if we normalize the amplitude with  $V_{tq}^* V_{tb}$  as usual, then

$$\left| \frac{V_{u^i s}^* V_{u^i b}}{V_{ts}^* V_{tb}} \right| \sim \begin{cases} O(\lambda^2) & , \quad u^i = u \\ O(1) & , \quad u^i = c \end{cases} , \quad (4)$$

for the former channel, and

$$\left| \frac{V_{u^i d}^* V_{u^i b}}{V_{td}^* V_{tb}} \right| \sim \begin{cases} O(1) & , \quad u^i = u \\ O(1) & , \quad u^i = c \end{cases} , \quad (5)$$

for the later one.  $\lambda$  is a parameter in Wolfenstein parametrization of CKM matrix [7] and the world average is  $\lambda \sim 0.22$  [12].

Involving the continuum as well as resonances parts of  $u\bar{u}$  and  $c\bar{c}$  loops, and NLO QCD correction into the calculation gives,

$$C_9^{\text{eff}} = C_9^{\text{NLO}} \left[ 1 + \frac{\alpha_s(\mu)}{\pi} \omega(\hat{s}) \right] + C_9^{\text{con}}(\hat{s}) + C_9^{\text{res}}(\hat{s}) , \quad (6)$$

where

$$C_9^{\text{con}}(\hat{s}) = \left[ \left( 1 + \frac{V_{uq}^* V_{ub}}{V_{tq}^* V_{tb}} \right) g(\hat{m}_c, \hat{s}) - \frac{V_{uq}^* V_{ub}}{V_{tq}^* V_{tb}} g(\hat{m}_u, \hat{s}) \right] \\ \times (3C_1 + C_2 + 3C_3 + C_4 + 3C_5 + C_6)$$

$$\begin{aligned}
& -\frac{1}{2}g(1, \hat{s}) (4C_3 + 4C_4 + 3C_5 + C_6) \\
& -\frac{1}{2}g(0, \hat{s}) (C_3 + 3C_4) + \frac{2}{9} (3C_3 + C_4 + 3C_5 + C_6) , \tag{7}
\end{aligned}$$

$$\begin{aligned}
C_9^{\text{res}}(\hat{s}) &= -\frac{16\pi^2}{9} (3C_1 + C_2 + 3C_3 + C_4 + 3C_5 + C_6) \\
&\times \left[ \left( 1 + \frac{V_{uq}^* V_{ub}}{V_{tq}^* V_{tb}} \right) \sum_{V=\psi, \dots} F_V(\hat{s}) - \frac{V_{uq}^* V_{ub}}{V_{tq}^* V_{tb}} \sum_{V=\rho, \omega} F_V(\hat{s}) \right] . \tag{8}
\end{aligned}$$

Here the NLO QCD correction has been given by A. J. Buras et.al. in [6], and

$$\begin{aligned}
\omega(\hat{s}) &= -\frac{2}{9}\pi^2 - \frac{4}{3}\text{Li}_2(\hat{s}) - \frac{2}{3}\ln \hat{s} \ln(1 - \hat{s}) - \frac{5 + 4\hat{s}}{3(1 + 2\hat{s})} \ln(1 - \hat{s}) \\
&- \frac{2\hat{s}(1 + \hat{s})(1 - 2\hat{s})}{3(1 - \hat{s})^2(1 + 2\hat{s})} \ln \hat{s} + \frac{5 + 9\hat{s} - 6\hat{s}^2}{6(1 - \hat{s})(1 + 2\hat{s})} , \tag{9}
\end{aligned}$$

represents the  $O(\alpha_s)$  correction from the one gluon exchange in the matrix element of  $\mathcal{O}_9$ . The function  $g(\hat{m}_{u^i}, \hat{s})$  which describes the continuum part of  $u^i \bar{u}^i$  pair contribution is,

$$\begin{aligned}
g(\hat{m}_{u^i}, \hat{s}) &= -\frac{8}{9} \ln \left( \frac{m_b}{\mu} \right) - \frac{8}{9} \ln(\hat{m}_{u^i}) + \frac{8}{27} + \frac{16}{9} \frac{\hat{m}_{u^i}^2}{\hat{s}} - \frac{2}{9} \left( 2 + \frac{4\hat{m}_{u^i}^2}{\hat{s}} \right) \sqrt{\left| 1 - \frac{4\hat{m}_{u^i}^2}{\hat{s}} \right|} \\
&\times \left[ \Theta \left( 1 - \frac{4\hat{m}_{u^i}^2}{\hat{s}} \right) \left( \ln \frac{1 + \sqrt{1 - 4\hat{m}_{u^i}^2/\hat{s}}}{1 - \sqrt{1 - 4\hat{m}_{u^i}^2/\hat{s}}} - i\pi \right) \right. \\
&\quad \left. + \Theta \left( \frac{4\hat{m}_{u^i}^2}{\hat{s}} - 1 \right) 2 \arctan \frac{1}{\sqrt{4\hat{m}_{u^i}^2/\hat{s} - 1}} \right] , \tag{10}
\end{aligned}$$

$$g(0, \hat{s}) = \frac{8}{27} - \frac{8}{9} \ln \left( \frac{m_b}{\mu} \right) - \frac{4}{9} \ln \hat{s} + \frac{4}{9} i\pi . \tag{11}$$

Remark that we put the relative phase in  $C_9^{\text{res}}$  to be zero due to unitarity constraint in the Argand plot of the transition amplitude (P. J. O'Donnel et.al. in [8]). On the other hand,  $F_V(\hat{s})$  is the Breit-Wigner resonance form,

$$F_V(\hat{s}) = \frac{\hat{f}_V^2(\hat{s})/\hat{m}_V^2}{\hat{s} - \hat{m}_V^2 + i\hat{m}_V\hat{\Gamma}_V} . \tag{12}$$

The parameter  $\hat{f}_V(\hat{s})$  which describes the momentum dependence of coupling strength of vector interaction in  $\gamma - V$  transition, i.e.

$$\langle 0 | \bar{u}^i \gamma_\mu u^i | V(q) \rangle \equiv f_V(q^2) \epsilon_\mu , \tag{13}$$

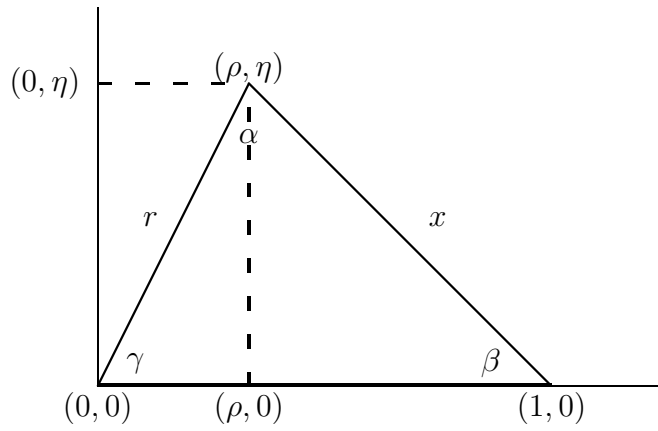


Figure 1: The CKM unitarity triangle on the  $\rho - \eta$  plane.

has been derived by K. Terasaki in [9] under an assumption that the vector-mesons are bound-states of the pair  $u^i \bar{u}^i$ , that is

$$\frac{\hat{f}_V(\hat{s})}{\hat{f}_V(0)} = 1 + \frac{\hat{s}}{\hat{P}_V} [P'_V - P''_V(\hat{s})] , \quad (14)$$

where

$$P''_V(\hat{s}) = \frac{\hat{m}_{u^i}^2}{4\pi^2 \hat{s}} \left[ -4 - \frac{5\hat{s}}{3\hat{m}_{u^i}^2} + 4 \left( 1 + \frac{\hat{s}}{2\hat{m}_{u^i}^2} \right) \sqrt{\frac{4\hat{m}_{u^i}^2}{\hat{s}} - 1} \arctan \frac{1}{\sqrt{4\hat{m}_{u^i}^2/\hat{s} - 1}} \right] , \quad (15)$$

is obtained from a dispersion relation involving the imaginary part of quark-loop diagram, while  $P_V$  and  $P'_V$  are the subtraction constants. Kinematically the above interpolation equation of  $f_V$  is valid only for  $0 \leq \hat{s} \leq \hat{m}_V^2$  region. For  $\hat{s} > \hat{m}_V^2$  region, we take same assumption with M. R. Ahmady in [9], that is  $\hat{f}_V(\hat{s} > \hat{m}_V^2) = \hat{f}_V(\hat{m}_V^2)$ . Then in principle, the ratio in Eq. (14) should be obtained from the known data of  $V$  production cross-section by off-shell and on-shell photons.

### 3 CKM unitarity triangle

Before going on examining the decay rate and asymmetries, let us give some relations in the CKM unitarity triangle as well as the numerical calculation for the auxiliary functions in the previous section. Especially it is worthwhile to see how large the contribution of CP violation terms in Eqs. (7) and (8) that can be collected as

Parameter	Value
$m_W$	$80.26 \pm 0.16$ (GeV)
$m_Z$	$91.19 \pm 0.002$ (GeV)
$m_u$	0.005 (GeV)
$m_d$	0.139 (GeV)
$m_c$	1.4 (GeV)
$m_b$	4.8 (GeV)
$m_t$	$175 \pm 9$ (GeV)
$m_e$	0.511 (MeV)
$m_\mu$	105.66 (MeV)
$m_\tau$	$1777^{+0.30}_{-0.27}$ (MeV)
$\mu$	$5^{+5.0}_{-2.5}$ (GeV)
$\Lambda_{QCD}^{(5)}$	$0.214^{+0.066}_{-0.054}$ (GeV)
$\alpha_{QED}^{-1}$	129
$\alpha_s(m_Z)$	$0.117 \pm 0.005$
$\mathcal{B}(B \rightarrow X_c l \bar{\nu})$	$(10.4 \pm 0.4)\%$
$\sin^2 \theta_w$	0.2325

Table 1: The values of parameters used throughout the paper.

$(V_{uq}^* V_{ub}/V_{tq}^* V_{tb}) C_9^{\text{CP}}(\hat{s})$ , with

$$\begin{aligned}
C_9^{\text{CP}}(\hat{s}) &= (3 C_1 + C_2 + 3 C_3 + C_4 + 3 C_5 + C_6) \\
&\times \left[ g(\hat{m}_c, \hat{s}) - g(\hat{m}_u, \hat{s}) - \frac{16 \pi^2}{9} \left( \sum_{V=\psi, \dots} F_V(\hat{s}) - \sum_{V=\rho, \omega} F_V(\hat{s}) \right) \right] \quad (16)
\end{aligned}$$

Using Wolfenstein parametrization [7], one can draw the unitarity triangle as Fig. 1 and then rewrite the CKM factor as,

$$\frac{V_{uq}^* V_{ub}}{V_{tq}^* V_{tb}} \sim \begin{cases} \frac{r (e^{-i\gamma} - r)}{1 + r^2 - 2 r \cos \gamma} & , \quad q = d \\ \lambda^2 r e^{-i\gamma} & , \quad q = s \end{cases} \quad (17)$$

where,  $r^2 = \rho^2 + \eta^2$  is the length of one side of the triangle and  $\gamma = \arctan(\eta/\rho)$  is one of the angle. As mentioned before, from Eqs. (4) and (17), thus it is obvious that in the  $b \rightarrow s \ell^+ \ell^-$  channel,  $u\bar{u}$  loop and then  $C_9^{\text{CP}}$  is less important and safely neglected.

Anyway, in general we must put  $r$  and  $\gamma$  as free parameters, while  $x$  must be determined by the data of  $B_d^0 - \bar{B}_d^0$  mixing. However, in the SM the unitarity

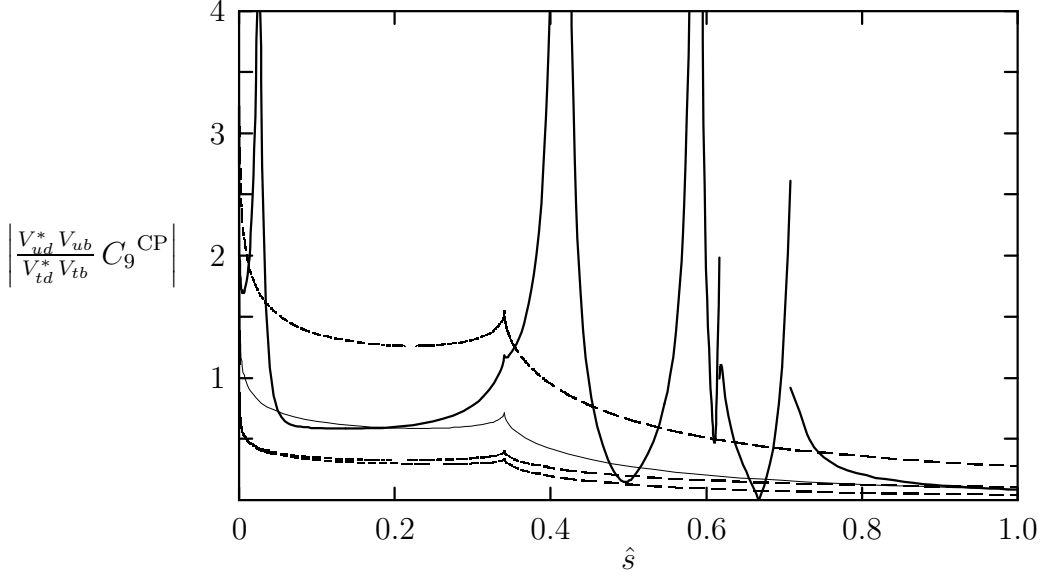


Figure 2: The magnitude of CP violation terms as a function of  $\hat{s}$  with (solid thick curve) and without (solid thin curve) LD contributions by putting  $(\gamma, x) = (48.6^\circ, 0.778)$ . The upper, middle and lower dashed curves are SD contribution only with same  $x$  but  $\gamma = 0, -\pi/2$  and  $\pi/2$ .

triangle is satisfied in a good approximation that make  $r$  and  $x$  should be related each other obviously. So remind that we have experimental value of  $x_d$  in  $B_d^0 - \bar{B}_d^0$  mixing process, that is  $x_d = 0.71 \pm 0.07$  [12]. From the CKM unitarity triangle, the length  $r$  can be expressed as,

$$r = \sqrt{|x^2 - \sin^2 \gamma|} + \cos \gamma, \quad (18)$$

where  $x$  is the length of opposite side of  $r$  and given as,

$$x = \left[ \frac{x_d}{G_F^2 / (6 \pi^2) m_{B_d} M_W^2 \tau_{B_d} \eta_{\text{QCD}} f_{B_d}^2 B_{B_d} |F_{\Delta B=2}|^2} \right]^{1/2}, \quad (19)$$

with [13],

$$F_{\Delta B=2} = \frac{4 - 15 x_t + 12 x_t^2 - x_t^3 - 6 x_t^2 \ln x_t}{4 (1 - x_t)^3}. \quad (20)$$

For the QCD correction factor  $\eta_{\text{QCD}}$ , we will use  $\eta_{\text{QCD}} = 0.55$ , while the world average for life-time of  $B^0$  is  $\tau_{B_d} = 1.28 \pm 0.06$  (ps).  $f_{B_d}^2 B_{B_d}$  is the parametrization of matrix element and we will take  $160 \leq \sqrt{f_{B_d}^2 B_{B_d}} \leq 240$  (MeV) from the conservative lattice calculation. Therefore, we obtain the value for  $x$ ,  $0.631 \leq x \leq 1.386$ .



Parameter	Vector-meson					
	$\rho$	$\omega$	$\psi$	$\psi'$	$\psi''$	$\psi'''$
$M_V$ (MeV)	768.5	781.94	3096.88	3686.00	3769.9	4040
$\Gamma_{e^+e^-}$ (keV)	6.77	0.6	5.26	2.14	0.26	0.75
$\Gamma_V$ (MeV)	150.7	8.43	0.087	0.277	23.6	52
$P_V''(\hat{m}_V^2)$	-0.00243	-0.00243	-0.02734	-0.01463	-0.01374	-0.01153
$\hat{P}_V$	0.01339	0.01387	0.01577	0.01830	0.01885	0.02080
$\hat{f}_V(0)$	0.00662	0.00202	0.01795	0.01487	0.00536	0.01010

Table 2: The experimental (central) values for the vector-mesons under consideration (upper table) and the determined constants under these values (lower table).

Further, using the central values of parameters given in Tab. (1), numerically we obtain the Wilson coefficients as

$$C_1 = -0.24038, C_2 = 1.10312, C_3 = 0.01069, C_4 = -0.02487, C_5 = 0.00720, \\ C_6 = -0.03023, C_7^{\text{eff}} = -0.31096, C_8 = 0.14778, C_9^{\text{NLO}} = 4.161, C_{10} = -4.54607.$$

The magnitude of  $(V_{ud}^* V_{ub}/V_{td}^* V_{tb}) C_9^{\text{CP}}$  as a function of  $\hat{s}$  is depicted in Fig. 2 for  $(\gamma, x) = (48.6^\circ, 0.778)$  that is the best fit in the SM up to now (solid curves) and equivalent to  $(\rho, \eta) = (0.3, 0.34)$ . It is clear that the contribution is significant, about  $\sim 20\%$  of  $C_9^{\text{NLO}}$  at low region of  $\hat{s}$  ( $< 0.4$ ) in the SM. The upper, middle and lower dashed curves show the magnitude when varying  $\gamma$  with 0 and  $\pi/2$ . Moreover, the dependence of  $C_9^{\text{CP}}$  on  $\eta$  is not as large as  $\rho$  that can be understood easily by evaluating Eq. (17).

Now, we can determine the values of the constants in Eq. (14) by using the data in Tab. (2), putting  $m_V \sim (2 m_{u^i})$  and  $P_V' = 0.043$  for all  $V$ 's. However, there is no data of photoproduction for others higher excited states of  $\psi$ , so let us use same average value  $|\hat{f}_V(0)/\hat{f}_V(\hat{m}_V^2)| \sim 0.35$  for  $V = \psi, \psi', \psi'', \psi'''$  and  $|\hat{f}_V(0)/\hat{f}_V(\hat{m}_V^2)| \sim 0.92$  for  $V = \rho, \omega$  which fit the data on  $\rho, \omega$  and  $\psi$  well [9]. This is also the reason why we do not consider resonances higher than  $\psi'''$ . Then we obtain the values of  $\hat{P}_V$  as written in Tab. 2. Otherwise,  $\hat{f}_V(\hat{m}_V^2)$  can be obtained from the data on

leptonic width [12], that is

$$\hat{f}_V^2(\hat{m}_V^2) = \frac{27 \hat{m}_V^3}{16 \pi \alpha^2} \hat{\Gamma}(V \rightarrow \ell^+ \ell^-), \quad (21)$$

then  $\hat{f}_V(0)$  would follow respectively as written in Tab. 2.

Now, we are ready to analyze the decay rate and asymmetries in the channel.

## 4 Decay rate and asymmetries

The double differential decay rate for semi-leptonic  $B \rightarrow X_q \ell^+ \ell^-$  decay, involving the lepton and light quark masses, can be expressed as,

$$\begin{aligned} \frac{d^2 \mathcal{B}(\hat{s}, z)}{d\hat{s} dz} &= \mathcal{B}_o \sqrt{1 - \frac{4 \hat{m}_\ell^2}{\hat{s}}} \hat{u}(\hat{s}) \left\{ 4 \left[ |C_9^{\text{eff}}|^2 - |C_{10}|^2 \right] \hat{m}_\ell^2 \left[ 1 - \hat{s} + \hat{m}_q^2 \right] \right. \\ &\quad + \left[ |C_9^{\text{eff}}|^2 + |C_{10}|^2 \right] \left[ (1 - \hat{m}_q^2)^2 - \hat{s}^2 - \hat{u}(\hat{s})^2 \left( 1 - \frac{6 \hat{m}_\ell^2}{\hat{s}} \right) z^2 \right] \\ &\quad + 4 |C_7^{\text{eff}}|^2 \frac{1 + 2 \hat{m}_\ell^2 / \hat{s}}{\hat{s}} \\ &\quad \times \left[ 1 - \hat{m}_q^2 - \hat{m}_q^4 + \hat{m}_q^6 - \hat{s} (8 \hat{m}_q^2 + \hat{s} + \hat{m}_q^2 \hat{s}) + \hat{u}(\hat{s})^2 (1 + \hat{m}_q^2) z^2 \right] \\ &\quad - 8 \text{Re} \left( C_9^{\text{eff}} \right)^* C_7^{\text{eff}} \left[ 1 + \frac{2 \hat{m}_\ell^2}{\hat{s}} \right] \left[ \hat{s} (1 + \hat{m}_q^2) - (1 - \hat{m}_q^2)^2 \right] \\ &\quad \left. + 4 C_{10} \left[ \text{Re} \left( C_9^{\text{eff}} \right)^* \hat{s} + 2 C_7^{\text{eff}} (1 + \hat{m}_q^2) \right] \hat{u}(\hat{s}) z \right\}, \quad (22) \end{aligned}$$

with  $\hat{u}(\hat{s}) = \sqrt{[\hat{s} - (1 + \hat{m}_q^2)][\hat{s} - (1 - \hat{m}_q^2)]}$ ,  $z = \cos \theta$  is the angle of  $\ell^+$  measured with respect to the  $b$ -quark direction in the dilepton CM system and the normalization factor,

$$\mathcal{B}_o = \mathcal{B}(B \rightarrow X_c \ell \bar{\nu}) \frac{3 \alpha^2}{16 \pi^2} \frac{|V_{tq}^* V_{tb}|^2}{|V_{cb}|^2} \frac{1}{f(\hat{m}_c) \kappa(\hat{m}_c)}, \quad (23)$$

is to reduce the uncertainties due to  $m_b$  and CKM factor, and in our notation it would read  $|V_{td}^* V_{tb}|^2 / |V_{cb}|^2 \sim \lambda^2 x^2$ .  $f(\hat{m}_c)$  is the phase space function for  $\Gamma(B \rightarrow X_c \ell \nu)$  in parton model, while  $\kappa(\hat{m}_c)$  accounts the  $O(\alpha_s)$  QCD correction to the decay.

Writing both functions explicitly,

$$f(\hat{m}_c) = 1 - 8 \hat{m}_c^2 + 8 \hat{m}_c^6 - \hat{m}_c^8 - 24 \hat{m}_c^4 \ln \hat{m}_c, \quad (24)$$

$$\kappa(\hat{m}_c) = 1 - \frac{2 \alpha_s(m_b)}{3 \pi} \left[ \frac{3}{2} + \left( \pi^2 - \frac{31}{4} \right) (1 - \hat{m}_c)^2 \right], \quad (25)$$

and using the values in Tab. 1,  $f(\hat{m}_c) = 0.538$  and  $\kappa(\hat{m}_c) = 0.884$ .

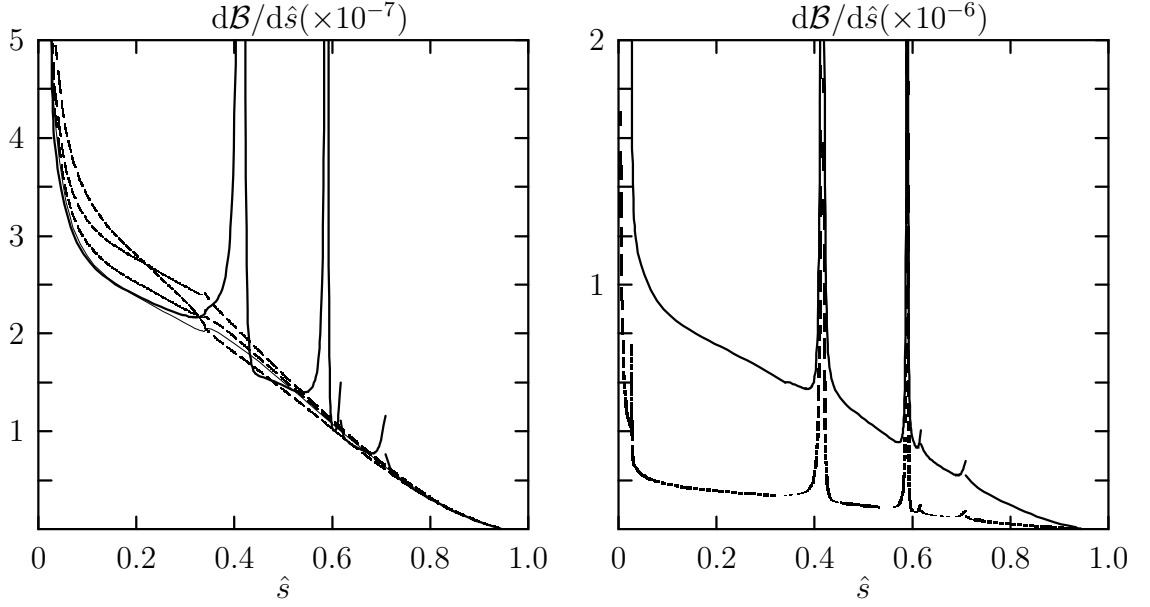


Figure 3: Left figure shows the differential BR of  $B \rightarrow X_d e^+ e^-$  as a function of  $\hat{s}$  with (thick curve) and without (thin curve) LD contributions by putting  $(\gamma, x) = (48.6^\circ, 0.778)$ . The upper, middle and lower dashed curves show the SD contribution with same  $x$  but  $\gamma = 0, \pi/2$  and  $-\pi/2$ . The right one shows the dependence on  $x$  with  $x = 1.368$  (solid curve) and  $0.631$  (dashed curve) and same  $\gamma$ .

#### 4.1 Decay rate

As a first step, let us consider the dilepton invariant mass distribution of the differential branching-ratio (BR) that is obtained by integrating Eq. (22) over the whole region of variable  $z$ ,

$$\frac{d\mathcal{B}(\hat{s})}{d\hat{s}} = \int_{-1}^1 dz \frac{d^2\mathcal{B}(\hat{s}, z)}{d\hat{s}dz}. \quad (26)$$

This gives the differential BR as follows,

$$\begin{aligned} \frac{d\mathcal{B}(\hat{s})}{d\hat{s}} = & \frac{4}{3} \mathcal{B}_o \sqrt{1 - \frac{4\hat{m}_\ell^2}{\hat{s}}} \hat{u}(\hat{s}) \left\{ 6 \left[ |C_9^{\text{eff}}|^2 - |C_{10}|^2 \right] \hat{m}_\ell^2 \left[ 1 - \hat{s} + \hat{m}_q^2 \right] \right. \\ & + \left[ |C_9^{\text{eff}}|^2 + |C_{10}|^2 \right] \left[ (1 - \hat{m}_q^2)^2 + \hat{s} (1 + \hat{m}_q^2) - 2\hat{s}^2 + \hat{u}(\hat{s})^2 \frac{2\hat{m}_\ell^2}{\hat{s}} \right] \\ & + 4 |C_7^{\text{eff}}|^2 \frac{1 + 2\hat{m}_\ell^2/\hat{s}}{\hat{s}} \\ & \times \left[ 2(1 + \hat{m}_q^2)(1 - \hat{m}_q^2)^2 - (1 + 14\hat{m}_q^2 + \hat{m}_q^4)\hat{s} - (1 + \hat{m}_q^2)\hat{s}^2 \right] \\ & \left. + 12 \text{Re} \left( C_9^{\text{eff}} \right)^* C_7^{\text{eff}} \left[ 1 + \frac{2\hat{m}_\ell^2}{\hat{s}} \right] \left[ (1 - \hat{m}_q^2)^2 - (1 + \hat{m}_q^2)\hat{s} \right] \right\}. \quad (27) \end{aligned}$$

The distributions of differential BR on dilepton invariant mass for  $B \rightarrow X_d e^+ e^-$  are given in Fig. 3. The large dependence on  $x$  is mostly coming from the overwhole

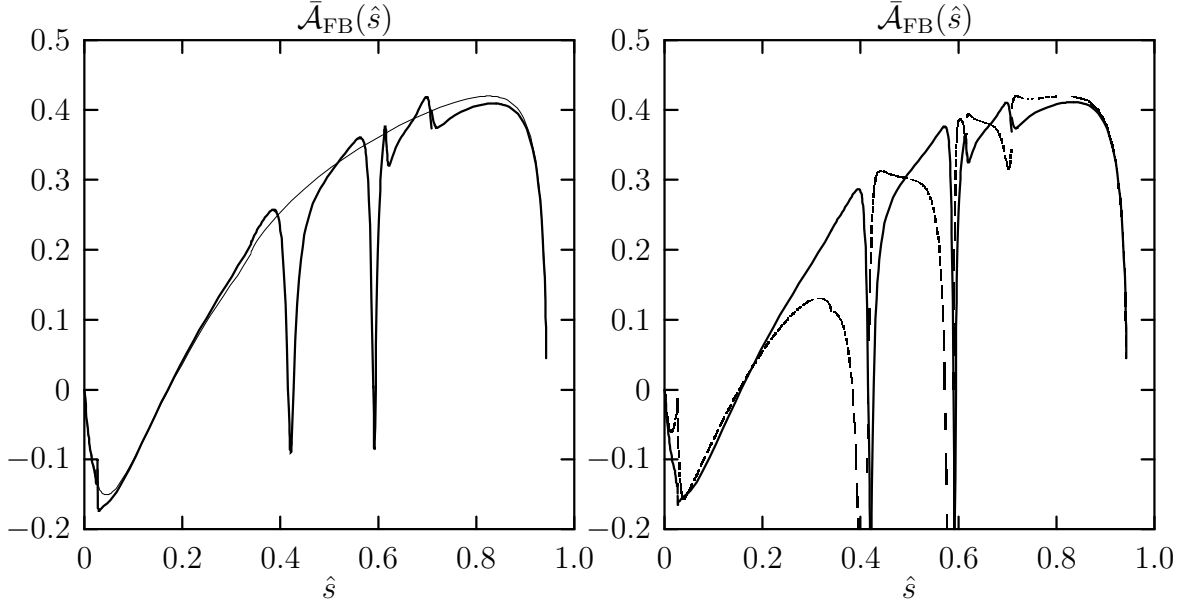


Figure 4: Left figure shows the differential FB asymmetry of  $B \rightarrow X_d e^+ e^-$  as a function of  $\hat{s}$  with (thick curve) and without (thin curve) LD contributions. The right one shows the dependence on  $\gamma$ , for  $\gamma = \pi/2$  (solid line) and 0 (dashed line).

CKM factor in Eq. (23), while the dependence on  $\gamma$  is significant only in the low  $\hat{s}$ . Thus, in the high  $\hat{s}$  region the differential BR may be a good test for  $x$  and then  $x_d$  obviously. In this meaning, it makes good the loss of  $B_d^0 - \bar{B}_d^0$  mixing due to the theoretical uncertainties in the treatment of hadron matrix element  $\langle B | \mathcal{O}^\dagger \mathcal{O} | B \rangle$ . Remind that, on the other hand the hadron matrix element in the inclusive  $B$  decays are theoretically under controlled. Anyway, we have also checked that the  $q$ -dependence of resonances in the channel is not as large as the case of  $B \rightarrow X_s e^+ e^-$  as pointed out by M. R. Ahmady in [9]. There is only  $\sim 4\%$  reduction compared with using  $\hat{f}_V(\hat{m}_V^2)$  for all region.

Next, we are going on examining some measurements that are sensitive to  $\gamma$  and less sensitive to  $x$ . This may be provided by considering the asymmetries and normalizing them with the differential BR, so the CKM factor proportioned to  $x$  will be cancelled.

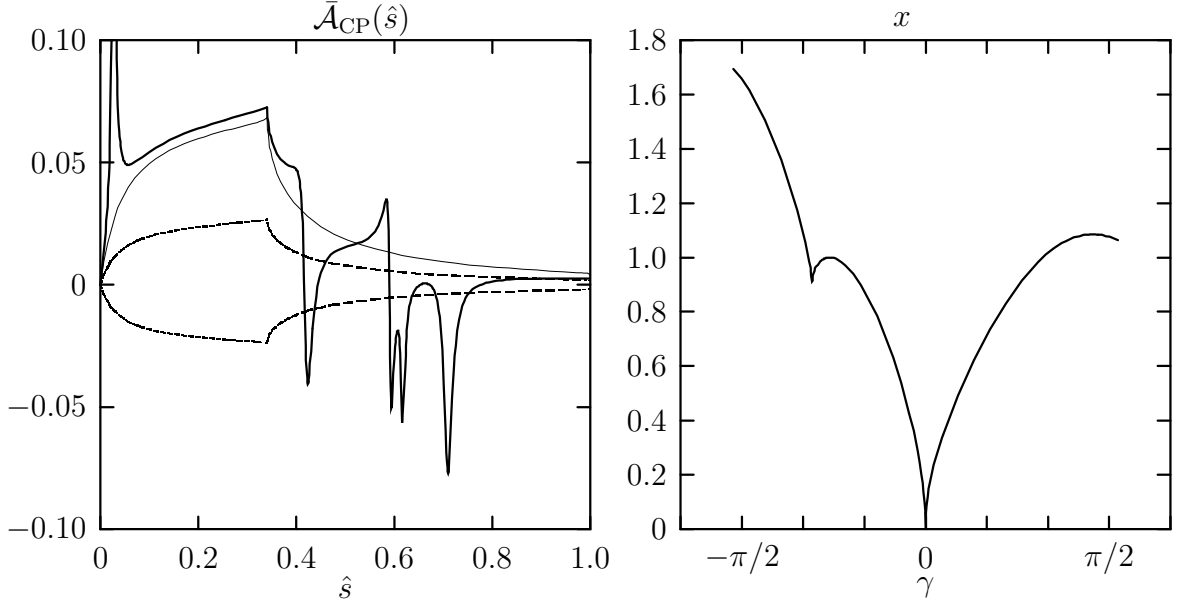


Figure 5: Left figure shows the differential CP asymmetry of  $B \rightarrow X_d e^+ e^-$  as a function of  $\hat{s}$  with (solid thick curve) and without (solid thin curve) LD contributions. The upper and lower dashed curves denote the SD contribution only with  $\gamma = \pi/2$  and  $-\pi/2$ . The right one shows  $x$  as a function of  $\gamma$  where  $\bar{\mathcal{A}}_{\text{CP}} = 0$ .

## 4.2 Forward-backward asymmetry

First, we provide the FB asymmetry. The normalized FB asymmetry is defined as follows [14],

$$\bar{\mathcal{A}}_{\text{FB}}(\hat{s}) = \frac{\int_0^1 dz \frac{d^2 \mathcal{B}(\hat{s}, z)}{d\hat{s} dz} - \int_{-1}^0 dz \frac{d^2 \mathcal{B}(\hat{s}, z)}{d\hat{s} dz}}{\int_0^1 dz \frac{d^2 \mathcal{B}(\hat{s}, z)}{d\hat{s} dz} + \int_{-1}^0 dz \frac{d^2 \mathcal{B}(\hat{s}, z)}{d\hat{s} dz}} = \frac{d\mathcal{A}_{\text{FB}}(\hat{s})/d\hat{s}}{d\mathcal{B}(\hat{s})/d\hat{s}}. \quad (28)$$

Then, after integrating Eq. (27) properly, the nominator reads,

$$\frac{d\mathcal{A}_{\text{FB}}(\hat{s})}{d\hat{s}} = -4 \mathcal{B}_o \sqrt{1 - \frac{4\hat{m}_\ell^2}{\hat{s}}} \hat{u}(\hat{s})^2 C_{10} \left[ \text{Re} \left( C_9^{\text{eff}} \right)^* \hat{s} + 2 C_7^{\text{eff}} \left( 1 + \hat{m}_q^2 \right) \right]. \quad (29)$$

In Fig. 4, we plot the differential FB asymmetry with and without the resonances in the left figure, while in the right one with varying  $\gamma$  and keep  $x$  to be constant.

## 4.3 CP asymmetry

By doing same treatment as done in [5] in the amplitude level, the normalized CP asymmetry can be written simply as,

$$\bar{\mathcal{A}}_{\text{CP}}(\hat{s}) = \frac{d\mathcal{B}(\hat{s})/d\hat{s} - d\bar{\mathcal{B}}(\hat{s})/d\hat{s}}{d\mathcal{B}(\hat{s})/d\hat{s} + d\bar{\mathcal{B}}(\hat{s})/d\hat{s}} = \frac{-2 d\mathcal{A}_{\text{CP}}(\hat{s})/d\hat{s}}{d\mathcal{B}(\hat{s})/d\hat{s} + 2 d\mathcal{A}_{\text{CP}}(\hat{s})/d\hat{s}}, \quad (30)$$

where  $\mathcal{B}$  and  $\bar{\mathcal{B}}$  denote the BR of the  $\bar{b} \rightarrow q \ell^+ \ell^-$  and its complex conjugate  $b \rightarrow \bar{q} \ell^+ \ell^-$  respectively. For convenience, let us divide  $C_9^{\text{eff}}$  to be two terms according to the factor  $V_{uq}^* V_{ub}/V_{tq}^* V_{tb}$  as below,

$$C_9^{\text{eff}} = \bar{C}_9 + \frac{V_{uq}^* V_{ub}}{V_{tq}^* V_{tb}} C_9^{\text{CP}}. \quad (31)$$

Then, the result for differential CP asymmetry is,

$$\begin{aligned} \frac{d\mathcal{A}_{\text{CP}}(\hat{s})}{d\hat{s}} &= \frac{4}{3} \mathcal{B}_0 \sqrt{1 - \frac{4\hat{m}_\ell^2}{\hat{s}}} \hat{u}(\hat{s}) \text{Im} \left[ \frac{V_{uq}^* V_{ub}}{V_{tq}^* V_{tb}} \right] \\ &\times \left\{ \text{Im} [\bar{C}_9^* C_9^{\text{CP}}] \left[ (1 - \hat{m}_q^2)^2 + \hat{s} (1 + \hat{m}_q^2) - 2\hat{s}^2 + \hat{u}(\hat{s})^2 \frac{2\hat{m}_\ell^2}{\hat{s}} \right. \right. \\ &\quad \left. \left. + 6\hat{m}_\ell^2 (1 - \hat{s} + \hat{m}_q^2) \right] \right. \\ &\quad \left. + 6 \text{Im} [C_7^{\text{eff}} C_9^{\text{CP}}] \left[ 1 + \frac{2\hat{m}_\ell^2}{\hat{s}} \right] [(1 - \hat{m}_q^2)^2 - (1 + \hat{m}_q^2) \hat{s}] \right\}. \quad (32) \end{aligned}$$

In Fig. 5, we give the distribution of  $\bar{\mathcal{A}}_{\text{CP}}$  in the dilepton invariant mass (left figure) with (solid thick line) and without the resonances (solid thin line). The upper, middle and lower dashed lines in the right figure show the SD contribution without resonances with  $\gamma = \pi/2, 0$  and  $-\pi/2$ . It is easily understood that in the present case the dependence on  $\gamma$  is quite large, because of the appearance of factor  $r \sin \gamma$  in Eq. (32). From the equation, it is clear that  $\bar{\mathcal{A}}_{\text{CP}}$  will be non-zero if the imaginary part of Eq. (17) is non-zero. Anyway, the condition that  $\bar{\mathcal{A}}_{\text{CP}} = 0$  for  $q = d$  in the SM is satisfied by the following equation,

$$x^2 = \sin^2 \gamma \left[ 1 + \frac{1}{4} \left( 1 - \sqrt{|3 + 4 \cot \gamma|} \right)^2 \right], \quad (33)$$

by using Eq. (18). The right figure in Fig. 5 is depicted based on this equation. Therefore, for the present data of  $x$ ,  $0.631 < x < 1.368$ , there are still allowed regions of  $\gamma$  where  $\bar{\mathcal{A}}_{\text{CP}} = 0$ . Notice again that from Eq. (17),  $\bar{\mathcal{A}}_{\text{CP}}(B \rightarrow X_s \ell^+ \ell^-)$  would be  $\sim 5\%$  of  $\bar{\mathcal{A}}_{\text{CP}}(B \rightarrow X_d \ell^+ \ell^-)$  due to the suppression of  $\lambda^2$ .

#### 4.4 Lepton-polarization asymmetry

Until now, we are considering the measurements that are less sensitive to the lepton mass. Next, let us going on providing the LP asymmetry which must be considered

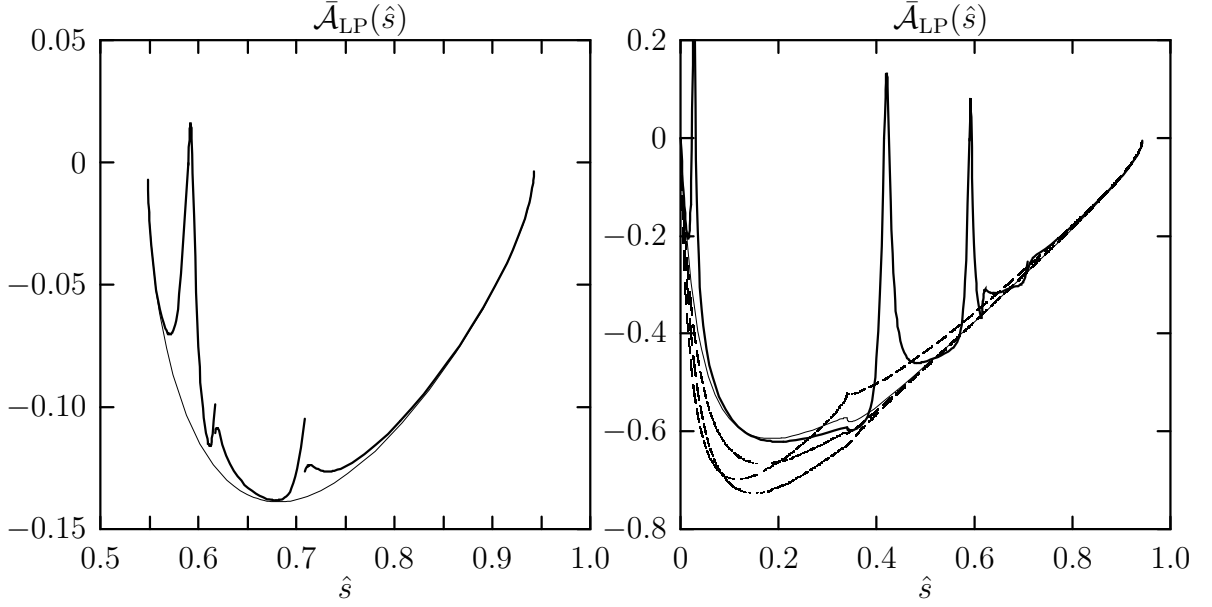


Figure 6: Left figure shows the differential LP asymmetry in the  $B \rightarrow X_d \tau^+ \tau^-$  as a function of  $\hat{s}$  with (solid thick curve) and without (solid thin curve) LD contributions. The right one is same but in the  $B \rightarrow X_d \mu^+ \mu^-$  case, the dashed curves denote the SD contribution with  $\gamma = 0, \pi/2$  and  $-\pi/2$ .

for heavy dilepton final state and is proposed first by J. L. Hewett in [15] for  $B \rightarrow X_s \tau^+ \tau^-$ . Generally, the normalized LP asymmetry is given as,

$$\bar{\mathcal{A}}_{\text{LP}}(\hat{s}) = \frac{d\mathcal{B}(\hat{s}, \mathbf{n})/d\hat{s} - d\mathcal{B}(\hat{s}, -\mathbf{n})/d\hat{s}}{d\mathcal{B}(\hat{s}, \mathbf{n})/d\hat{s} + d\mathcal{B}(\hat{s}, -\mathbf{n})/d\hat{s}} = \frac{d\mathcal{A}_{\text{LP}}(\hat{s})/d\hat{s}}{d\mathcal{B}(\hat{s})/d\hat{s}}, \quad (34)$$

with  $\mathbf{n}$  is a unit vector of any given spin direction of  $\ell^-$  in the  $\ell^-$  rest frame. Then, for the longitudinal polarization, that is  $\mathbf{n}$  has same direction with the momentum of  $\ell^-$  ( $\mathbf{p}_{\ell^-}$ ),

$$\begin{aligned} \frac{d\mathcal{A}_{\text{LP}}(\hat{s})}{d\hat{s}} &= \frac{8}{3} \mathcal{B}_o \left( 1 - \frac{4\hat{m}_\ell^2}{\hat{s}} \right) \hat{u}(\hat{s}) C_{10} \left\{ 6 C_7^{\text{eff}} \left[ (1 - \hat{m}_q^2)^2 - \hat{s} (1 + \hat{m}_q^2) \right] \right. \\ &\quad \left. + \text{Re} \left( C_9^{\text{eff}} \right)^* \left[ (1 - \hat{m}_q^2)^2 + \hat{s} (1 + m_q^2) - 2\hat{s}^2 \right] \right\}. \end{aligned} \quad (35)$$

However, for  $\tau^+ \tau^-$  final state the dependence on  $\gamma$  is tiny. This is because, as shown in Fig. 6, in the channel there is only the distribution for  $\hat{s} > (4\hat{m}_\tau^2)$ , while generally the large dependence is expected for low  $\hat{s}$ . It is obvious that the situation in the present case is similar as in the FB asymmetry by comparing Eqs. (29) and (35). So it may be interesting to consider the transversal polarization, that has different structure (F. Krüger et.al. in [15]). Unfortunately, we have also checked

that the measurement of transversal lepton polarization asymmetry is too small for light dilepton like  $\mu^+\mu^-$ , then we must consider  $\tau^+\tau^-$  that the distribution is limited for higher region of  $\hat{s}$  which should not be altered by varying  $\gamma$  as mentioned above.

## 5 Summary and discussion

We have shown how to extract the angle  $\gamma$  of CKM unitarity triangle by the inclusive  $B \rightarrow X_d \ell^+ \ell^-$  decay as well as the data of  $x_d$  in the SM. From the channel it is possible to get independent information to examine the unitarity triangle. The information should be very important to test the SM as well as determine the discrepancies between the theory and the experimental data that may open the window to beyond the SM.

As results, finally we can make some points as below.

1. For low  $\hat{s}$  region, i.e.  $0.1 < \hat{s} < 0.3$ , 5  $\sim$  10% discrepancies in the  $\mathcal{B}(B \rightarrow X_d e^+ e^-)$  and  $\bar{\mathcal{A}}_{\text{LP}}(B \rightarrow X_d \mu^+ \mu^-)$  may be good signals for the CP violation factor defined here.
2. From the fact that the dependence of  $\gamma$  in the high  $\hat{s}$  region, i.e.  $\hat{s} > 0.6$ , is tiny, a precise measurement of  $x_d$  can also be done by exploring one of the measurements discussed in the present paper in addition to the present data from  $B_d^0 - \bar{B}_d^0$  mixing and the future radiative  $B \rightarrow X_d \gamma$  decay.
3. A trivial CP violation asymmetry in  $B \rightarrow X_d e^+ e^-$  should measure the dependence on  $\gamma$ . It will, at least, be a good probe to determine the sign of the angle  $\gamma$ .

## Acknowledgements

The author thanks to M. R. Ahmady, T. Morozumi and Y. Kiyo for useful discussion in  $1/q^2$  dependence in long distance effects and the  $q$ -dependence of  $V - \gamma$  transition. The author also would like to thank Particle Elementer Physics Group for the warm hospitality during the stay at ICTP, Italy in the last part of the



work. The work is supported by a grant from the Ministry of Education, Science and Culture, Japan.

## References

- [1] A. Ali, talk given at 4th KEK Topical Conference on Flavor Physics in Tsukuba - Japan, and references therein.
- [2] B. Grinstein, M. J. Savage and M. B. Wise, *Nucl. Phys.* **B319** (1989) 271;  
R. Grigjanis, P. J. O'Donnell, M. Sutherland and H. Navelet, *Phys. Lett.* **B223** (1989) 239.
- [3] A. V. Manohar and M. B. Wise, *Phys. Rev.* **D49** (1994) 1310;  
A. Ali, G. Hiller, L. T. Handoko and T. Morozumi, *Phys. Rev.* **D55** (1997) 4105.
- [4] T. Morozumi, in *private communications*.
- [5] F. Krüger and L. M. Sehgal, *Phys. Rev.* **D55** (1997) 2799.
- [6] M. Jezabek and J. H. Kühn, *Nucl. Phys.* **B320** (1989) 20;  
M. Misiak, *Nucl. Phys.* **B393** (1993) 23 [Err. **B439** (1995) 461];  
A. J. Buras and M. Münz, *Phys. Rev.* **D52** (1995) 186.
- [7] L. Wolfenstein, *Phys. Rev. Lett.* **51** (1983) 1945.
- [8] C. S. Lim, T. Morozumi and A. I. Sanda, *Phys. Lett.* **B218** (1989) 343;  
N. G. Deshpande, J. Trampetic and K. Panose, *Phys. Rev.* **D39** (1989) 1461;  
P. J. O'Donnell and H. K. K. Tung, *Phys. Rev.* **D43** (1991) R2067;  
P. J. O'Donnell, M. Sutherland and K. K. Tung, *Phys. Rev.* **D46** (1992) 4091.
- [9] K. Terasaki, *Nuo. Cim.* **66A** (1981) 475;  
N. G. Deshpande, X. G. He and J. Trampetic, *Phys. Lett.* **B367** (1996) 362;  
M. R. Ahmady, *Phys. Rev.* **D53** (1996) 2843.
- [10] C. D. Lü and D. X. Zhang, *Phys. Lett.* **B397** (1997) 279.

- [11] T. Inami and C. S. Lim, *Prog. Theor. Phys.* **65** (1981) 297.
- [12] Particle Data Group, *Phys. Rev.* **D54** (1996) 1.
- [13] A. J. Buras and M. K. Harlander, in *Heavy Flavours* (World Scientific, 1992) p. 58, edited by A. J. Buras and M. Lindner.
- [14] A. Ali, T. Mannel and T. Morozumi, *Phys. Lett.* **B373** (1991) 505.
- [15] J. L. Hewett, *Phys. Rev.* **D53** (1996) 4964;  
F. Krüger and L. M. Sehgal, *Phys. Lett.* **B380** (1996) 199.